Research Square

Preprints are preliminary reports that have not undergone peer review.
They should not be considered conclusive, used to inform clinical practice,
or referenced by the media as validated information.

# Functionality and safety of an abdominal vagus nerve electrode for chronic implantation and stimulation in mice

**Rustha Kalenther**
The University of Melbourne
**Tomoko Hyakumura**
Bionics Institute
**Jenny Zhou**
Bionics Institute
**James Fallon**
Bionics Institute
**Sophie Payne**
spayne@bionicsinstitute.org

Bionics Institute

**Research Article**

**Keywords:**

**Posted Date:** November 17th, 2026

**DOI:** https://doi.org/10.21203/rs.3.rs-11641617/v1

**License:** This work is licensed under a Creative Commons Attribution 4.0 International License.
Read Full License

**Additional Declarations:** Competing interest reported. Sophie Payne and James Fallon are Associate Editors for Bioelectronic Medicine.

# Functionality and safety of an abdominal vagus nerve electrode for chronic implantation and stimulation in mice

Rustha Kalenther[1,2], Tomoko Hyakumura[1,2,3], Jenny Zhou[1,3], James Fallon[1,2,3], Sophie Payne[1,2,3]

[1]The Bionics Institute of Australia, East Melbourne, VIC, Australia
[2]Department of Medical Bionics, The University of Melbourne, Parkville, VIC, Australia
[3]Swinburne University of Technology, Victoria, Australia

Corresponding author:
Sophie Payne
35 Victoria Parade,
Daly Wing
St Vincent's Hospital
Fitzroy VIC 3065
spayne@bionicsinstitute.org

## Abstract

Electrical stimulation of the vagus nerve has emerged as a promising bioelectronic therapy for inflammatory and neurological disorders. However, an important step of translation is to assess efficacy of vagal nerve stimulation (VNS) in a range of mouse models of human disease. As such, this study evaluated the safety, functionality, and chronic performance of a cuff electrode array for implantation on the abdominal vagus nerve of awake, freely moving mice. A custom four-electrode platinum cuff was implanted on the abdominal vagus nerve of C57BL/6 mice for 28 days. Mice received no stimulation ($n$=4) or chronic VNS ($n$=9; 1.8 mA, 100 μs/phase, 10 Hz, 3 h/day, 5 days/week). All the electrodes from no VNS mice are referred to as passive electrodes (n=16). In stimulated mice, the electrode pair used to deliver stimulation is referred to as stimulated electrodes (n=18) and the electrode pair used for recording from the nerve is referred to as unstimulated electrodes (n=18). Electrochemical and electrophysiological measurements were taken pre- and post- chronic implantation and stimulation, and during 4 weeks of *in vivo* testing. There were no changes in the *in vitro* electrochemical impedance spectroscopy (EIS) and CIL of electrodes. Charge storage capacity of stimulated electrodes increased post implantation, potentially indicating changes to the electrode effective surface area. However, there were no significant increases in vitro of CSC values across all electrodes. Longitudinal *in vivo* measurement of EIS showed a Main effect of Time across all electrodes, likely due to tissue encapsulation. There were no differences in vivo CIL between stimulated, unstimulated and passive electrodes. However, the CG of stimulated electrodes was significantly lower than passive electrodes. ECAP thresholds in chronically stimulated mice were significantly higher than unstimulated mice ($p$ = 0.001). However, 100% of recorded electric thresholds (n=77 recordings from $n$=13 mice) remained below Shannon electrical safety limit (Shannon safety parameter k=1.75) and the water separation window (216 μC/cm$^2$/phase). Stimulation was well tolerated in awake mice, and there were no differences ($p \geq 0.05$) in vagal fascicle area from nerves taken from normal, no VNS and chronic VNS mice. Together, data show the abdominal vagus nerve cuff electrode is a safe platform for

chronic stimulation in mice and provides a valuable technology platform for investigating bioelectronic therapies in transgenic and disease-specific mouse models.

## Introduction

The human body uses bioelectricity as a mode of communication in the body. The peripheral nervous system (PNS) plays a key role in sending sensory and motor signals between the central nervous system (CNS) and other organs in the body [1]. The PNS is surgically accessible and has rich information as it has direct access to neural circuits that could be a great target to therapeutically intervene and treat a broad range of diseases [1]. The vagus nerve is the main autonomic nerve that emerges from the brainstem and innervates many vital organs [2]. It plays an important part in the brain-gut axis, bi-directionally communicating between the brain and the gut and is known to regulate heart rate, modulate respiration, appetite and digestion and recently shown to modulate the body's response to inflammation [3]. Cervical vagus nerve stimulation (VNS) is an FDA-approved therapy for drug-resistant epilepsy [4], treatment-resistant depression [5] and moderate-to-severe rheumatoid arthritis [6] and is in early clinical trials for the treatment of inflammatory bowel disease [7-9]. As such, the application for VNS as a therapy for human disease is growing rapidly. However, a critical step for translation is to generate robust efficacy studies using preclinical models of disease.

Historically, cervical VNS treatment has been associated with stimulation-induced effects on respiratory alterations, oxygen saturation [10], sleep disorders [11], voice alterations, paraesthesia, cough, dyspnoea, dysphagia and pain [12]. Such off-target effects are due to the activation of low threshold cervical vagal fibers to the larynx, pharynx, heart, and lungs. Significant efforts have been made to reduce stimulation-induced side effects by developing wireless VNS technology that delivers short bursts of stimulation (SetPoint Medical). However, an alternative solution is to stimulate the abdominal vagus nerve at a site below cardiac/pulmonary vagal branches.

Our laboratory's own efforts have demonstrated stimulation of the abdominal vagus nerve results in no changes to breathing, heart rate and blood pressure in rats [13,14], sheep [15] and humans (NCT05469607). Our recent efforts have shown efficacy of abdominal VNS in rat models of inflammatory bowel disease [14] and rheumatoid arthritis [16] which have recently led to two safety trials for these conditions (NCT05469607; NCT07017686). The translation of the abdominal VNS technology critically relied on the development of custom design electrode arrays appropriately sized for rat, sheep and human. However, to expand this abdominal VNS research further, the main aim of this study was to develop an abdominal VNS array for mice suitable for chronic implantation and stimulation.

Mice are the most used animal model in research as there are numerous genetically modified mouse disease models, and genetic modification of mouse is a well-established practice [17]. The shorter average life span and breeding time of mice makes it advantageous to study the slow progression of diseases in human over a short period [18,19]. Hence, an abdominal vagus nerve device for mice could be used in different mouse disease models that are similar to human diseases which support the translation of VNS therapy for a wide range of human diseases. However, the small mouse anatomy presents several challenges for electrode design. The average adult mouse size is 15-25g, which presents a challenge for weight of the percutaneous plugs and stiffness of cables in restricting natural movement. Furthermore, as the diameter of the abdominal vagus nerve of the mouse is 112 ± 9 μm [20] the nerve and adjacent tissues are very fragile, and the design of the electrode should be compatible with such delicate anatomy.

A final design requirement is the need for 2-pairs of electrodes to allow bipolar stimulation and recording of electrically evoked compound action potentials (ECAPs). This is an important feature in all our abdominal VNS experimental studies [14] as it allows unequivocal feedback that the vagus nerve has been activated. Due to these design requirements, this study developed an extraneural cuff electrode, to minimize damage to the nerve and surrounding tissues, with 2 pairs of platinum electrodes (**Figure 1**). Here we assessed the safety and biocompatibility of chronic implantation of our custom-made abdominal vagus nerve array over 28 days of implantation.

The main function of an implantable electrode array is to be able to safely deliver charge to the nerve during chronic implantation. Platinum and platinum-iridium are widely used electrode material due to its biocompatibility [21,22], reversible charge storage capacity [23,24] and resistance to corrosion [25] and is used clinically for many neuromodulation devices. A second aim of this study is to assess the safety of chronic stimulation, using the new device, on the abdominal vagus nerve. When safe levels of charge are passed from the electrode to neural tissue, reversible faradaic reactions are reversed by the charge-balanced bi-phasic pulse ensuring no net charge released into the biological environment [26]. However, when unsafe levels of charge are passed, irreversible faradaic reactions such as the electrolysis of water, corrosion of electrode material and chloride ion oxidation [27] occur causing pH changes [28] and tissue damage [26,29,30].

As such, here we surgically implanted mice with a custom-made abdominal vagus nerve electrode array for 28 days. Mice were randomly assigned to receive VNS stimulation of 180 nC/phase 3 hrs/day over 4 weeks, which was based on the upper level of maximum safe limits of the Shannon criteria (charge density per phase, and charge per phase, with a dimensionless parameter k= 1.75 [31,32]. Electrochemical characteristics of the electrodes pre/post implantation and *in vivo* were assessed, including charge injection limit (CIL), charge storage capacity (CSC), electrochemical impedance spectrometry (EIS) and cyclic voltammetry (CV) tests. Biological safety was assessed through observing animal behavior and histology of the chronically implanted and stimulated nerves was also assessed for signs of damage.

# Methods

### Design of a custom cuff four electrode array

*Design*: A new 4-platinum electrode cuff array was custom made for mice and based on previous designs for rats [14,33]. Due to size constrictions electrodes 1 and 2 (E1, E2, proximal, stimulating pair, **Figure 1A**) were implanted around the abdominal vagus nerve while electrode 3 and 4 (E3, E4, distal, recording pair or no stimulation, **Figure 1A**) were placed around the gastric branches of the vagus nerve (**Figure 1B)**. Platinum (Pt) electrodes (Pt-Ir (90/10) were made from 100 µm cross-sectional diameter Pt wire and give surface areas of 0.079 mm². Dimensions of the nerve cuff were determined by histological analysis of the anterior vagus nerve in normal mice ($n$ = 10; **Figure 1C**). The distance between adjacent electrodes (E1–E2, or E3–E4, center to center) was 0.5 mm and the distance between adjacent pairs of electrodes (center to center) was 4.5 mm (**Figure 1A**). Electrodes were placed in a medical grade silicone cuff, and a silicon tube (OD of 0.6 mm x ID of 0.3 mm) protected the helical cable as it traversed to a percutaneous pedestal magnetic connector [34]. Two reinforced silicon tabs were positioned opposite the nerve channel to allow suturing to the esophagus. The magnetic connector was made of a pedestal and external connector with 3D printed framework, flex PCB and N50

neodymium magnet. Multi strength PTFE insulated Pt-Ir (90/10) wire (150 µm in diameter) coiled for return was attached to the pedestal end.

*Array cleaning*: Arrays were sonicated prior to chronic implantation through a cycle of Pyroneg/distilled water for 15 minutes, double distilled water rinses of 5 minutes each, 96% ethanol rise for 10 minutes followed by two rinses in distilled water for 5 minutes each. Arrays were then sterilized using an autoclave. At the end of chronic implantation, arrays were run through the same sonication cleaning cycle [33].

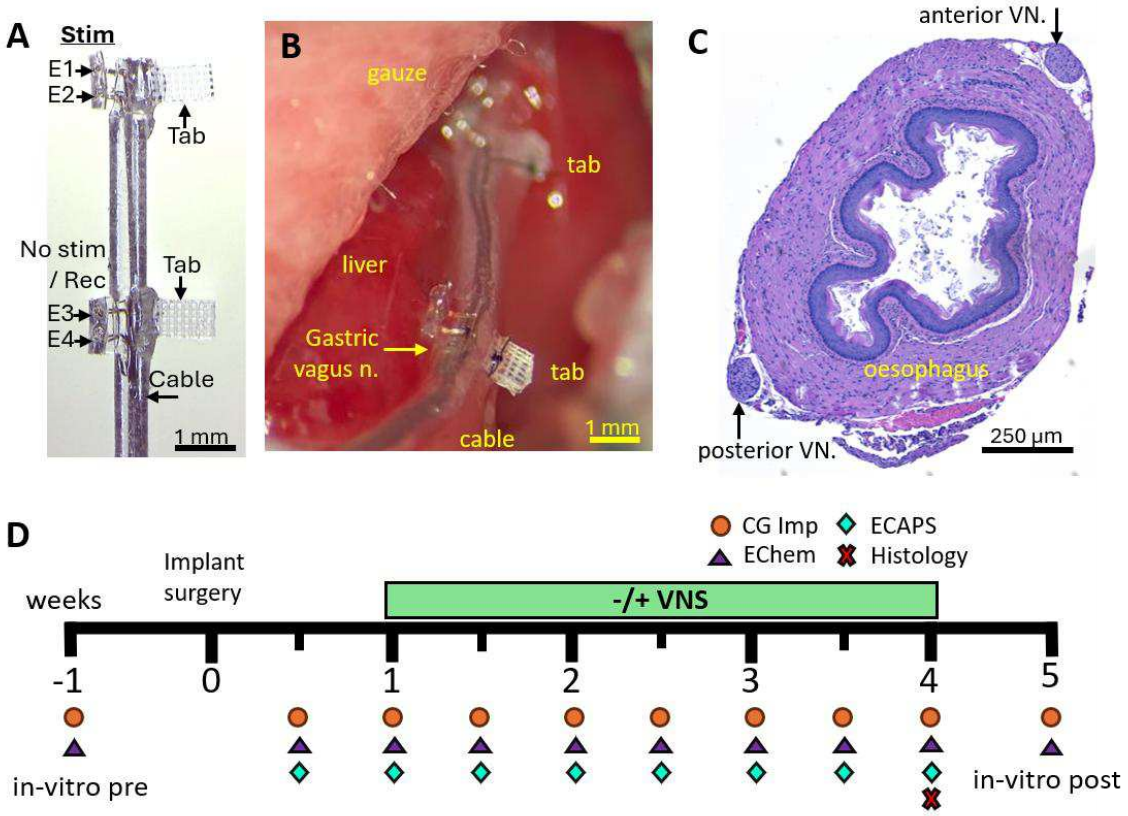



***Figure 1***. *Vagus nerve electrode array design, placement* in vivo*, histology of the implant site and in vivo experimental schedule.* ***A****: image of the 4-platinum cuff electrode array designed for the abdominal vagus nerve of the mouse. In mice that received VNS, the stimulating pair of electrodes was E1 and E2, and the no stimulation electrodes, also used for recording, were E3 and E4.* ***B****: An* in vivo *image taken during implantation surgery of the abdominal vagus nerve array and cuffed vagus nerve. The image also shows gauze used to retract the liver, and tabs used to suture the array to the underlying esophagus.* ***C****: Image of an H&E stained cross-section of the esophagus with the attached anterior and posterior vagus nerves.* ***D****: Schematic diagram of the experimental timeline unstimulated (No VNS) and stimulated (VNS) animal cohorts. All animals were implanted for 28 days total and routinely underwent awake testing for: common ground impedance (CG Imp), electrochemistry (EChem: EIS, CV, CIL) recorded through a 2-cell setup and electrically evoked compound action potentials (ECAPs). After 1 week of recovery, mice were randomly assigned to receive no VNS or VNS (3 hours/day, 5 days/week). On day 28, mice were terminated and implanted vagal tissues taken for histology. Abbreviations: EIS: electrochemical impedance spectroscopy; CV: cyclic voltammetry; CIL: charge injection limit.*

**Bench-top *in vitro* common ground impedance and electrochemical measurements**

*Common ground impedance*: was measured in saline prior to surgery and following post dissection cleaning through sonication processes. Biphasic current (100 μA, 100 μs) pulses were passed between an electrode of interest and all other electrodes using a custom stimulator [35]. The peak voltage at the end of the first phase (Vtotal) of the current pulse was measured, and the Vtotal value was used to calculate total common ground (CG) impedance (Ztotal) using Ohm's law (Z = voltage/current).

*Electrochemical measurements:* were performed pre- and post- chronic implantation following cleaning via sonication. Electrodes from the mouse array were used as working electrodes, a Pt electrode served as the counter and an Ag|AgCl served as a reference. 3-cell electrode set up was used for the *in vitro* electrochemical measurements in saline [36]. EIS and CV were performed using a potentiostat (Gamry Instruments, Interface 1000$^{TM}$). EIS was done with the frequency value ranging from 1 to 100 kHz with the AC voltage of 50 mV rms at 10 points/decade. CV was performed by cycling the electrode potential between -0.6 and 0.8 V at a scan rate of 150 mV/s for 5 cycles. The average of cycles 2-5 was determined and then the area under the average CV curve was integrated to obtain CSC. The CIL is the maximum charge that can be injected before water electrolysis takes place at the maximum cathodic potential -0.6V [26]. The maximum CIL was obtained using a pulse width of 100 μs by increasing the current amplitudes from 100 μA until it reached the cathodal polarization limit of -0.6 V, up to a maximum current output of the stimulator 2mA. Description of electrochemical in vivo testing is described later in the methods section.

**Animal cohorts, experimental schedule and electrode groups**

*Animal cohorts*: A normal group (*n*=10) of mice did not receive implants and were used to generate histological data of the abdominal vagus nerve to inform upon the device design (**Figure 1A, C**). Experimental implant cohorts (Supplementary Table 1) consisted of:

- **i)** unstimulated animals (No VNS; *n*=4), in which mice received an implant, were tethered and handled in the same way as a stimulated animal but received no VNS;
- **ii)** stimulated animals (VNS *n*=9) in which mice received active VNS for 3 hrs/day.

*Experimental schedule*: Bench-top electrochemical measurements of the vagus nerve electrode arrays were made pre- and post-implantation. As described in **Figure 1D**, following implantation surgery, all implanted mice underwent testing for *in vivo* electrochemistry, common ground impedance and ECAPs twice a week for 4 weeks. After 4 weeks of implantation, final electrophysiology tests were done under non-recovery anesthesia, then mice were terminated and tissue taken for histological assessment of damage (**Figure 1C, D**).

*Group of electrodes*: The electrodes are classified into three groups for analysis:

- **i)** Passive electrodes (*n*=16) refer to all electrodes from no VNS mice (*n*=4);
- **ii)** No-stimulation (no stim *n*=18) electrodes are unstimulated electrodes E3 and E4 from VNS mice (*n*=9)
- **iii)** Stimulated electrodes (stim *n*=18) are electrodes E1 and E2 from VNS mice (*n*=9).

**Animals and anesthesia**

This study used a total of 23 male wildtype (C57BL/6) mice (8-9 weeks old, Breeding Research Centre, Walter and Elisa Hall Institute of Medical Research, Victoria, Australia) at an average weight of 25.33 ± 1.63 g (mean ± standard deviation) at the time of surgery. All procedures were approved by Animal Ethics Committee of St. Vincent's Hospital, Melbourne, (applications: #004/21 and #013/24) and complied with the Australian Code for the Care and Use of Animals for Scientific Purposes (National Health and Medical Research Council of Australia) and the Prevention of Cruelty to Animals (1986) Act. Mice implanted with a device

were housed individually to avoid damage to implants but were provided with environmental enrichment. Mice were kept under a 12 h light/dark cycle and allowed *ad libitum* access to standard chow and water. For implantation surgery, mice were anesthetized (1-2% isoflurane and 1L/min of oxygen flow) and given general (0.05 mg/kg of 0.01 mg/L buprenorphine, subcutaneous injection) and local analgesia (1 mg/kg of 5 mg/L bupivacaine, subcutaneous injection) at the incision sites. At the end of the 4-week implantation period, mice were anesthetized (1-1.5% isoflurane and 1L/min of oxygen flow) for a non-recovery end of life experiment in which electrophysiology tests were performed and mice euthanized (300mg/kg Lethabarb, intraperitoneal injection).

**Implantation surgical procedure**

Implantation of the device was similar to that described for rats [33]. In short, the liver was retracted to expose the anterior abdominal and gastric vagus nerve (**Figure 1B**). The proximal electrode pair (E1 – E2) was implanted around the abdominal vagus nerve and the distal pair (E3 – E4) around a gastric branch (**Figure 1A, B**). Sutures were used to anchor the array to the esophagus to hold in place. The return electrode was placed subcutaneously on the lead wire and an exteriorized magnetic percutaneous plug placed on the dorsal lumbar aspect of the animal [34].

**Electrophysiological recordings and analysis**

*Recordings:* ECAP recordings were always taken before electrochemical *in vivo* testing and before chronic stimulation. ECAPs were measured using a custom stimulator, bipolar stimulation (10 Hz, 200 μs, 0-2 mA, 50 repetitions in 2 repeats) applied to proximal electrodes (E1-E2; **Figure 1A**). Bipolar recordings were made from distal electrodes (E3-E4; **Figure 1A**) and evoked activity amplified (ISO-80, World Precision Instruments, USA), recorded (sampled at 200 kHz; USB-6211, National Instruments, USA), digitally filtered (200–3000 Hz band pass) and visualised using IGOR Pro-9 software (IGOR v9.0, Wavemetrics, USA).

*Analysis*: ECAP threshold from the abdominal – gastric vagus nerve was defined as the minimum current required to evoke a waveform 0.1 μV above baseline levels (2.25–15 ms) [37]. The current level required to evoke an ECAP i.e. ECAP threshold was used to calculate the charge per phase (Q) and charge density per phase (D), which was plotted on the Shannon graph [32] to check if the abdominal VNS device functions within the safe limits of stimulation. Charge per phase (Q) was calculated by multiplying the maximum threshold current by the pulse width of the stimulating current and the charge density per phase (D) was calculated by dividing the charge per phase (Q) by the surface area of the electrode.

***In vivo* common ground impedance and electrochemical testing**

*Common ground impedance*: was measured as *in vitro testing* mentioned above twice/week over the 4 weeks of chronic implantation. All measurements were done while the mice were awake and moving in the cage.

*Electrochemical testing*: Open circuit electrodes were excluded from electrochemical analysis for all following time-points. The EIS, CV, CIL and CG of the electrodes were measured using 2-cell electrode set-up over 4 weeks implantation period (**Figure 1C**). The equipment and procedures for the electrochemical measurements were similar to *in vitro* measurements, with the exceptions that the EIS was done with the frequency value ranging from 100 Hz to 100 kHz with the AC voltage of 50mV rms, and the final frequency was increased to 100 Hz from 1 Hz used in *in vitro* measurements to avoid any tissue damage (Dalrymple, Huynh et al. 2020).

**Chronic stimulation**

Mice selected to receive stimulation (VNS: $n$=9) were stimulated for 3 hrs/day, 5 days/week using charge balanced bi-phasic pulses of 180 μC (100 μs per phase, 50 μs interphase gap, 1.8 mA) at 10 Hz delivered to proximal electrodes (E1, E2). Unstimulated (No VNS) mice received no stimulation (0 μC, 3 h/day, 5 days/week).

**Histological processing, analysis and imaging**

On completion of the 4-week chronic study, mice were euthanized and perfused transcardially with 0.9 % saline and 10% neutral buffered formalin (NBF) in 0.1 M phosphate buffer, pH 7.4. The esophagus, abdominal vagus nerve, implanted array and other attached tissues were removed together and post-fixed in 10% NBF for 24 hours and later washed 3 times in 0.1 M phosphate buffered saline (PBS). Similar to previous studies [14], the vagus nerve contained within proximal electrodes E1-E2 was marked with tissue dye (Davidson Marking System®, Trajan Scientific and Medical, Vic, Australia). The esophagus and attached dye-marked abdominal vagus nerve was embedded in paraffin and serial cross sections stained with hematoxylin and eosin (H&E) and imaged for histopathological analysis of damage. An observer (SCP) blinded to experimental conditions used H&E-stained sections to evaluate the degree of mechanical and/or electrical damage to the abdominal vagus nerve, and the adjacent esophagus, associated with electrodes 1 and 2 (E1, E2) from chronically implanted No VNS and VNS cohorts. At electrode location E1-E2, light microscope images were taken using a Zeiss Axioplan II microscope and Axiovision software (Zeiss, Germany). Total fascicle cross-sectional area was quantified across one representative section per electrode position per animal, using FIJI (Open-Source image processing and analysis software, Fiji.sc [38]).

**Statistical Analysis**

Details of each statistical test are stated in the relevant results section. In brief, bench top testing of common ground impedance and electrochemistry measures (EIS, CV, CIL, CSC) before and after chronic implantation were assessed using a two-way RM ANOVA (Time x Electrode condition). Differences across Time (pre vs. post) or between electrodes (passive, stim and no-stim) were assessed using a Tukey's *post hoc* test. All longitudinal *in vivo* differences in impedance measurements, ECAPs, electrochemical measures (EIS, CV, CIL, CSC) or histological changes were assessed using one-way or two-way RM ANOVA or Mixed Effect Model (repeated measures for Time) with appropriate *post hoc* tests, stated in the results. Statistically significant differences were accepted as $p$-values $\leq 0.05$, and GraphPad Prism 10 (GraphPad Software, United States) or Igor Pro 9 (WaveMetrics, Inc. Portland, USA) used for all analysis.

# Results

## Histological dimensions for array design

Histological dimensions of the anterior and posterior vagus nerve, and underlying esophagus, were acquired ($n$=10) (**Figure 1C**; **Table 2**) and dimensions used in the electrode array development (**Figure 1A**). The area of the abdominal vagus nerve was 0.008 ±0.001 $mm^2$, the abdominal nerve width was 130 ± 7.0 µm while the range of fascicle numbers was between 1-2 (mean: 1.8 ±0.29 fascicles). The width of the esophagus was 961.9 ± 33 µm and the circumference was 3339 ± 92.6 µm.

## Bench-top electrochemical measurements before and after chronic implantation and stimulation

Bench-top electrochemical properties (EIS, CSC, CIL) using a 3-cell electrode set up, as well as CG impedance, were performed on passive ($n$=16), no stimulation ($n$=16) and stimulated ($n$=16) electrodes (**Table 2**) before and after chronic implantation (**Figure 2**). Differences between the three electrode groups and between pre- and post-implantation were analyzed using a two-way RM ANOVA (Time x Electrode Condition). Differences across Time (pre vs. post) or between Electrode Conditions were assessed using a Tukey's *post hoc* test.

*In vitro* EIS

A representative graph across 1 to 100 kHz frequencies is shown from one passive, one no stim and one stim electrode both pre- and post-implantation (**Figure 2A**). A group analysis of all electrodes from each group was performed at 1 Hz (**Figure 2B**), 1 kHz (**Figure 2C**) and 10 kHz (**Figure 2D**), indicated in **Figure 2A** by black dotted lines. At 1 Hz (**Figure 2B)**, the impedance magnitude pre-implantation across all electrode groups was approximately 3,563 ± 1,071 kΩ and 3,437 ± 698 kΩ following chronic implantation. Analysis shows there was no significant interaction of time and electrode condition ($F_{(2,35)} = 0.17$, $p = 0.85$), no main effect of Time ($F_{(1,35)} = 0.02$, $p = 0.9$) and no main effect of Electrode condition ($F_{(2,35)} = 2.9$, $p = 0.07$) in passive, no stim and stim electrodes, indicating stable low frequency impedance between electrode groups. Similarly, at 1 kHz (**Figure 2C**) the impedance magnitude pre-implantation across all electrode groups was approximately 11.1 ± 3.3 kΩ and 12.2 ± 2.7 kΩ following chronic implantation. Analysis shows there was no significant interaction between time and electrode condition ($F_{(2,35)} = 0.46$, $p = 0.64$), no main effect of Time ($F_{(1,35)} = 0.1$, $p = 0.75$) and no main effect of Electrode condition ($F_{(2,35)} = 2.4$, $p = 0.11$) in passive, no stim and stim electrodes, indicating stable medium frequency impedance between electrode groups. Finally, at 10 kHz (**Figure 2D**) the impedance magnitude pre-implantation across all electrode groups was approximately 2.8 ± 0.52 kΩ and 2.5 ± 0.51 kΩ following chronic implantation. Analysis shows there was no significant interaction between time and electrode condition ($F_{(2,35)} = 0.73$, $p = 0.49$), no main effect of Time ($F_{(1,35)} = 0.32$, $p = 0.57$) and no main effect of Electrode condition ($F_{(2,35)} = 1.96$, $p = 0.16$) in passive, no stim and stim electrodes, indicating stable high frequency impedance between electrode groups.

*In vitro* CSC

A group analysis of charge storage capacity, the resultant measurable factor from CV, indicated the mean pre-implantation CSC across all electrode groups was 2.6 ± 0.33 µC/cm², while post CSC values were 2.9 ± 0.32 µC/cm². Analysis shows there was a significant interaction between Time x Electrode Condition ($F_{(2,35)} = 4.34$, $p = 0.021$; **Figure 2E**), but no significant main effects of Time ($F_{(1,35)} = 1.01$, $p = 0.32$) and Electrode Condition ($F_{(2,35)} = 1.71$, $p = 0.39$). Post-hoc analysis of the Time x Electrode condition interaction indicated these significant changes were driven by a significant increase between pre- and post-implantation CSC values in stim electrodes ($p = 0.006$).

*In vitro* CIL

The average CIL across all electrode groups pre-implantation was 53.3 ± 2.14 mC/cm², and 63.0 ± 5.1 mC/cm² post-implantation (**Figure 2F**) Analysis shows there was no significant interaction ($F_{(2,38)} = 0.83$, $p = 0.44$), no main effect of Time ($F_{(1,38)} = 2.00$, $p = 0.17$) and no main effect of Electrode condition ($F_{(2,38)} = 0.42$, $p = 0.66$) in passive, no stim and stim electrodes, indicating a stable CIL for all electrodes in all conditions.

In vitro CG impedance

The pre-implantation CG impedance across all electrode groups was approximately 9.5 ± 0.86 kΩ and 9.3 ± 1.14 kΩ following chronic implantation. Analysis shows there was no significant interaction between Time x Electrode Condition ($F_{(2,41} = 0.17$, $p = 0.84$) and no significant main effect of Time ($F_{(1,42)} = 0.06$, $p = 0.81$; **Figure 2G**). However, there was a significant effect of Electrode Condition ($F_{(2,41)} = 3.91$, $p = 0.028$). A *post hoc* test on the Main Effects of Electrode Condition shows passive electrode CG impedance was significantly higher than no stim electrodes ($p = 0.03$; **Figure 2G**) and showed a non-significant trend higher than stim electrodes ($p = 0.077$). Data indicates no effects of Time, therefore differences are likely driven by overall manufacturing differences of electrodes.

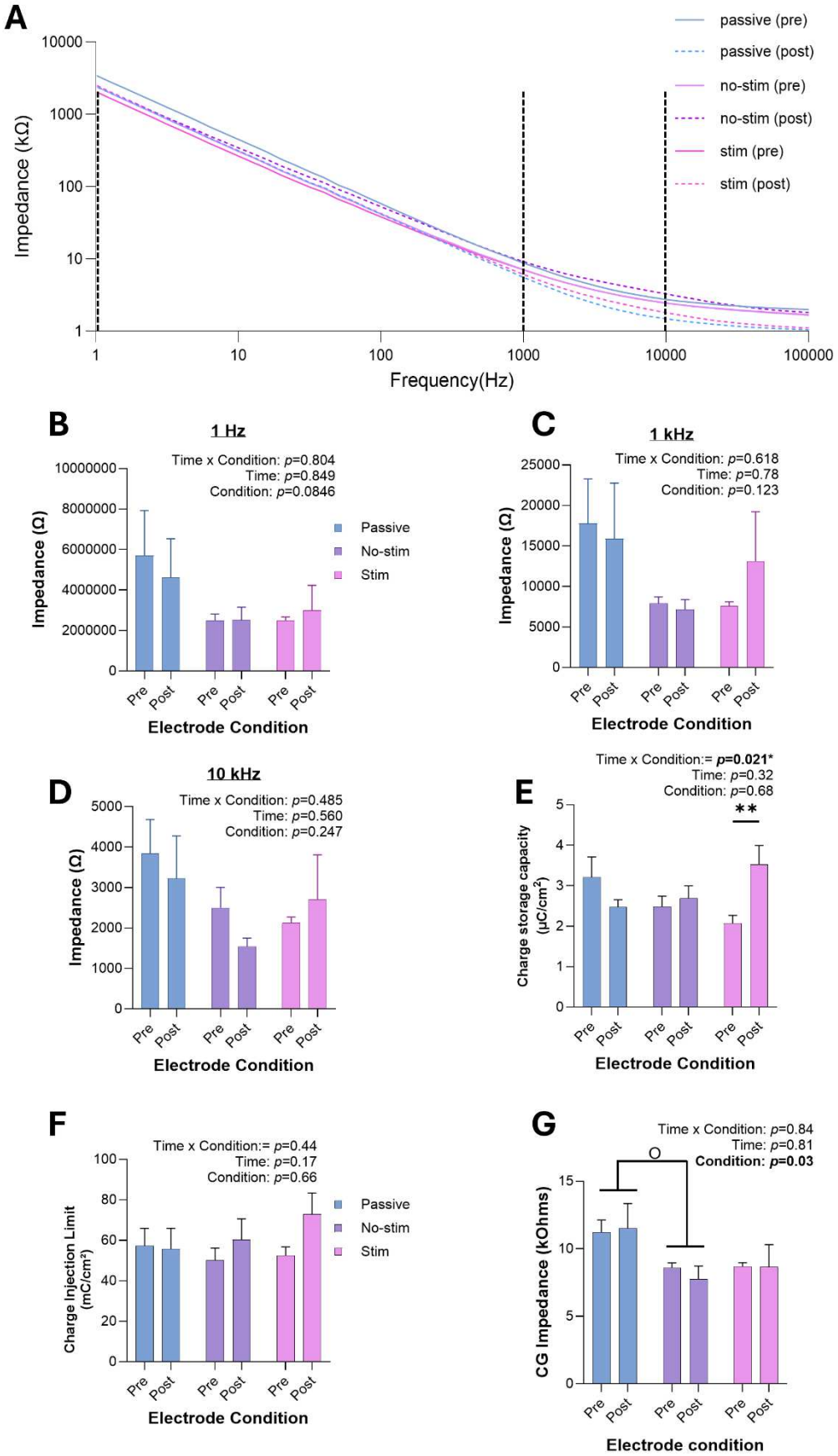



***Figure 2**. Bench-top electrochemical recordings before implantation (pre) and after chronic implantation and stimulation measured via 3-electrode cell set up. **A**: Representative*

*electrochemical impedance spectroscopy (EIS) impedance from a passive, no stim and stim electrode across frequencies from 1 Hz – 100 kHz. Grouped analysis was conducted at frequencies 1 Hz, 1 kHz and 10 kHz, indicated by black dotted lines.* ***B-D****: Graphs show analysis of impedance at 100 Hz (B), 1 kHz (C) and 10kHz (D).* ***E****: Graph of storage capacity (CSC).* ***F****: Graph of charge injection limit (CIL).* ***G****: Graph of common ground impedance (CG impedance). Data in B to G show mean ± SEM. A two-way RM ANOVA was performed between Time X Electrode and significance accepted as p<0.05. In* ***F****, significant differences between pre- and post-CSC values were indicated as '*'. In* ***G****, Main Effects between electrode condition was indicated by 'O'.*

**Electrochemical *in vivo* performance during chronic implantation and electrical stimulation**

Electrochemical properties (EIS, CSC, CIC), as well as CG impedance, of passive ($n$=16), no stim ($n$=18) and stim ($n$=18) electrodes were assessed *in vivo* using a 2-cell electrode set up in awake freely moving mice twice a week over 4 weeks. Analysis was conducted on data over 4 weeks (**Figure 3, 4**). Differences between passive, no stim and stim (Electrode Condition) groups and over Time were analyzed using a Mixed Effects Model (Time x Electrode Condition) due to missing values in the longitudinal data set (**Figure 3, 4**). Differences between Electrode Conditions between passive electrode values and other groups were assessed using a Dunnett's *post hoc* test. Differences over Time between 0.5 weeks (pre-stim baseline) and all other timepoints were assessed using a Dunnett's *post hoc* test.

<u>*In vivo* EIS</u>

A representative graph across 100 Hz to 100 kHz frequencies is shown from one passive, one no stim and one stim electrode at week 0 and week 4 following chronic implantation (**Figure 3A**). Group analysis of all electrodes from each group was performed at 100 Hz (**Figure 3B**), 1 kHz (**Figure 3C**) and 10 kHz (**Figure 3D**), indicated by black dotted lines in Figure 3A.

At 100 Hz (**Figure 3B)**, the impedance magnitude at week 0.5 across all electrode groups was approximately 72.9 ± 6.10 kΩ. Analysis shows there was no significant interaction ($F_{(0.21, 4.1)}$ = 1.6, $p$ = 0.162), and no main effect of Electrode Condition ($F_{(2,45)}$ =2.56, $p$ = 0.087). However, there was a significant main effect of Time ($F_{(11, 4.1)}$ = 14.5, $p$ = 0.030). A Main Effect of Time Dunnett's post hoc analysis showed that 100 Hz impedance of all electrodes was significantly less than 0.5 week (baseline) at 1 week ($p$ = 0.015), 1.5 weeks ($p$ < 0.0001), 2 weeks ($p$ < 0.0001), 2.5 weeks ($p$ = 0.0002), 3 weeks ($p$ < 0.0001), 3.5 weeks ($p$ = 0.013) and 4 weeks ($p$ = 0.0006).

At 10 kHz (**Figure 3C)**, the impedance magnitude at week 0.5 across all electrode groups was approximately 17.2 ± 1.4 kΩ. Analysis shows there was no significant interaction ($F_{(0.47, 9.1)}$ = 3.2, $p$ = 0.111), no main effect of Electrode Condition ($F_{(2,45)}$ = 2.35, $p$ = 0.110) and no main effect of Time ($F_{(0.24, 9.1)}$ = 5.9, $p$ = 0.059). At 10 kHz (**Figure 3D)**, the impedance magnitude at week 0.5 across all electrode groups was approximately 9.0 ± 0.95 kΩ. Analysis shows there was no significant interaction ($F_{(2.3, 43.9)}$ = 3.0, $p$ = 0.051), and no main effect of Electrode Condition ($F_{(2,45)}$ =1.2, $p$ = 0.319). However, there was a significant main effect of Time ($F_{(1.1, 43.9)}$ = 8.0, $p$ = 0.005). A Main Effect of Time Dunnett's post hoc analysis showed that 100 Hz impedance of all electrodes were significantly higher than 0.5 week (baseline) values at 1.5 weeks ($p$ = 0.006), 3 weeks ($p$ = 0.024), and 4 weeks ($p$ = 0.004).

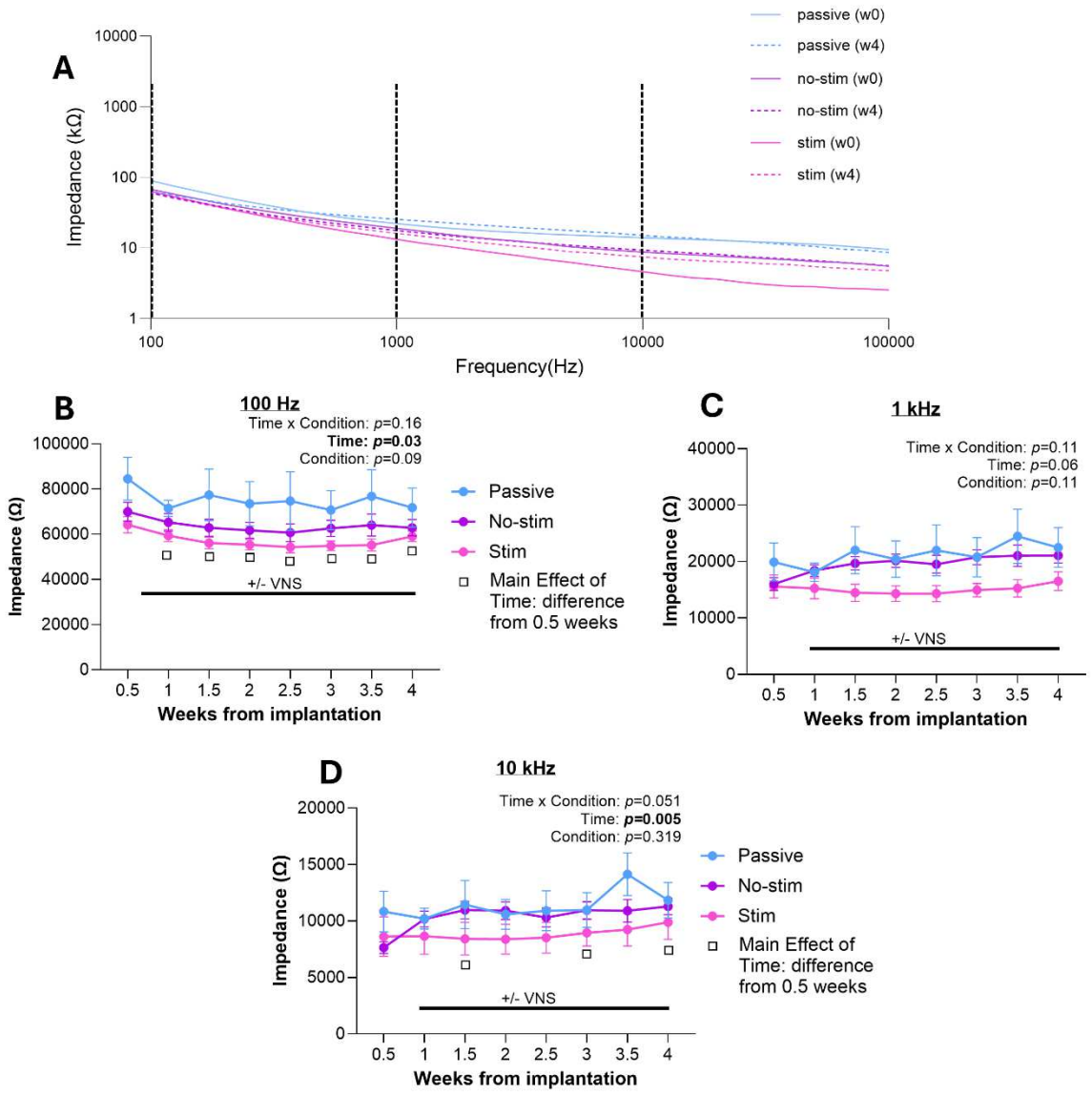



***Figure 3***. *Electrochemical recordings in vivo during chronic implantation and stimulation.* ***A****: Representative electrochemical impedance spectroscopy (EIS) impedance from a passive, no stim and stim electrode across frequencies from 1 Hz – 100 kHz over 4 weeks. Analysis was performed at 100 Hz, 1 kHz and 10 kHz, indicated by black dotted line.* ***B-D****: Graphs show group analysis of impedance at 100 Hz (B), 1 kHz (C) and 10 kHz (D)over 4 weeks of chronic implantation and stimulation. Data in B, C, D show mean ± SEM. A Mixed Effects Model was performed between Time X Electrode and significance accepted as p<0.05. Main Effect of Time differences across all electrodes from the 0.5 w value within an electrode condition was indicated by a square black box.*

<u>*In vivo* CIL</u>

There was a significant interaction between Time X Electrode Condition on in vivo CIL ($F_{(2.1, 89.8)} = 2.5$; $p = 0.048$), a significant Main Effect of Time ($F_{(2.1, 89.8)} = 4.91$; $p = 0.009$) and a significant Main Effect of Electrode condition ($F_{(2, 49)} = 4.7$; $p = 0.013$; **Figure 4A)**. Owing to significant interaction between Time × Electrode, a *post hoc* analysis of the interaction was performed. The interaction was driven by a significant decrease (compared to 0.5 week baseline

CIL values) in no stim electrodes on weeks 1 ($p$ = 0.03), week 1.5 ($p$ = 0.02), week 2 ($p$ = 0.007), week 3 ($p$ < 0.001), week 3.5 ($p$ = 0.0004) and 4 ($p$ = 0.0002), but no change reported at 2.5 weeks ($p$ = 0.099; **Figure 4A**). In stim electrodes, CIL values significantly increased in week 2 ($p$ = 0.04), compared to week 0.5 baseline values. However, the CIL of passive electrodes remained unchanged over the 4 weeks ($p \geq 0.05$), compared to 0.5 weeks CIL values. Notably, there were no significant differences between passive electrode CIL, no stim or stim values over the 4 weeks.

*In vivo* CG impedance

There was a significant interaction between Time X Electrode Condition on in vivo CG impedance ($F_{(12, 286)} = 5.1$; $p < 0.0001$), a significant Main Effect of Time ($F_{(6, 286)} = 15.4$; $p<0.0001$) and a significant Main Effect of Electrode condition ($F_{(2,49)} = 14.4$; $p < 0.0001$; **Figure 4B)**. Owing to significant interaction between Time × Electrode, a *post hoc* analysis of the interaction was performed. The interaction was driven the passive electrode CG significant increase at week 2 ($p$ = 0.014) and 3.5 weeks ($p$ = 0.023; **Figure 4B**, differences indicated by solid blue square), compared to 0.5 weeks. The no stim electrode CG significantly increased on week 1 ($p$ = 0.0054), week 1.5 ($p$ = 0.0002), week 2 ($p$ = 0.0002), week 3 ($p$ < 0.0001), week 3.5 ($p$ < 0.0001) and week 4 ($p$ < 0.0001; **Figure 4B**, differences indicated by open purple square). However, stim electrode CG impedance remained unchanged over 4 weeks ($p \geq 0.05$). The interaction was also driven by passive electrode CG being significantly higher than no stim electrodes at week 0.5 ($p$ = 0.05) and week 2 ($p$ = 0.02), (**Figure 4B**, differences indicated by purple'*'). Passive electrode CG was significantly higher than stim electrode CG at week 0.5 (0.048), week 1.5 ($p$ = 0.001), week 2 ($p$ < 0.0001), week 2.5 ($p$ = 0.0024), week 3.5 ($p$ < 0.0001), week 4 ($p$ = 0.0002) (**Figure 4B**, differences indicated by cross-in-circle symbol).

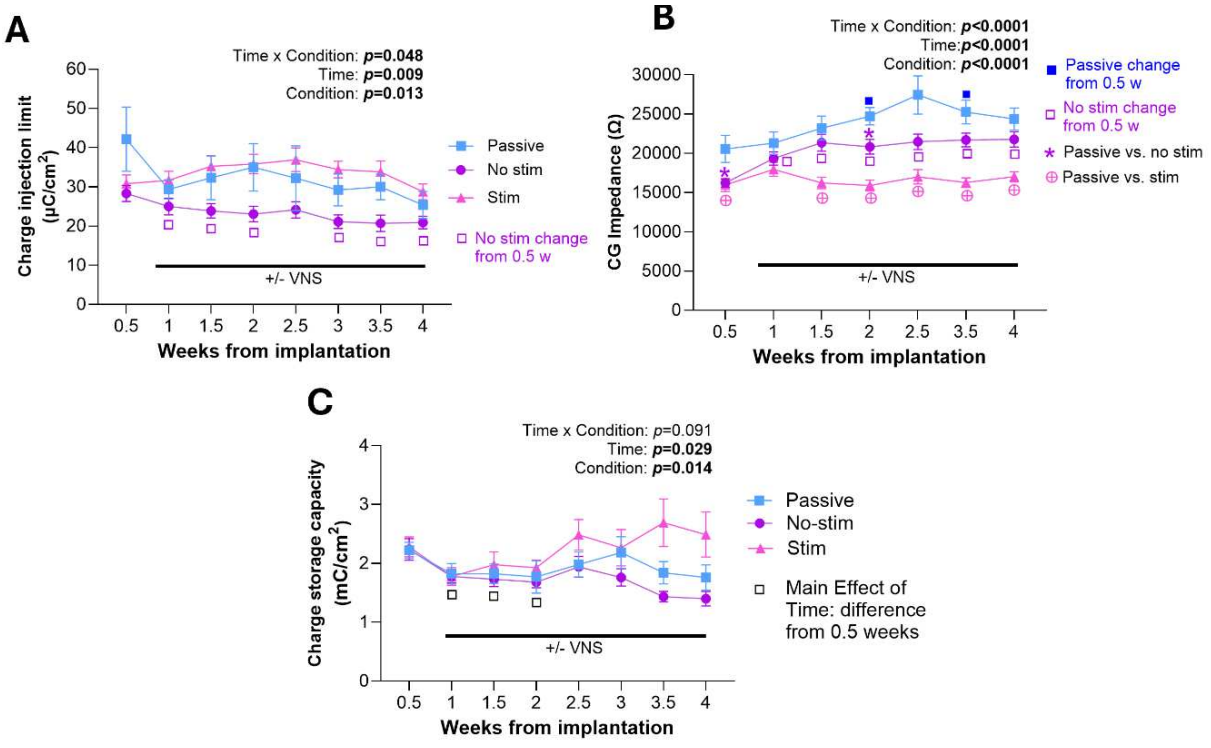



***Figure 4****. Changes in charge injection limit and common ground impedance in vivo during 4 weeks of chronic implantation and stimulation.* ***A****: Graph of charge injection limit from passive (n=16), no stim (n=18) and stim (n=18) electrodes from unstimulated and stimulated mice.* ***B****: Graph of CG impedance from electrodes of unstimulated and stimulated mice.* ***C****:*

*Graph of CSC from electrodes of unstimulated and stimulated mice. Data in all graphs show mean ± SEM, and a Mixed Effect Model was performed between Time X Stimulation, and significance was accepted as p<0.05. Dunnett's post hoc test was performed on the interaction to assess differences between 0.5 weeks and subsequent weeks, and between passive electrode CG values and others.*

*In vivo* CSC

There was no significant interaction between Time X Electrode Condition on *in vivo* CSC ($F_{(8.0, 152)} = 1.8$; $p = 0.091$); however, there was a significant Main Effect of Time ($F_{(4.0, 152)} = 2.8$; $p = 0.03$) and a significant Main Effect of Electrode condition ($F_{(2, 45)} = 4.7$; $p = 0.014$; **Figure 4C)**. A Dunnett's *post hoc* test on the Main Effects of Time on all electrodes showed a significant transient decrease in CSC at week 1 ($p = 0.004$), week 1.5 ($p = 0.02$) and week 2 ($p = 0.008$), compared to baseline values at 0.5 weeks. Despite the significant Main Effect of Electrode condition, Dunnett's *post hoc* tests revealed no significant differences in pairwise comparisons (**Figure 4C**). Nevertheless, as apparent in Figure 4C, there was a trend towards an increase in CSC for the Stim electrodes, consistent with the *in vitro* results in Figure 2E.

**Changes in electrically evoked compound action potentials during chronic implantation and stimulation**

ECAPs were successfully recorded during week 4 in 9 of 11 chronically implanted mice (**Table 1**). Specifically, $n$=4 of 4 unstimulated mice had ECAPs during week 4, while $n$=7 of 9 stimulated mice had ECAPs in the fourth week of testing. Representative ECAPs from a chronically stimulated mouse ($n$=1) are shown in Figure 5, with the activation threshold at 300 µA on week 0 (**Figure 5A**) and 1300 µA at week 4 (**Figure 5B**). During the entire chronic implantation and stimulation period, the maximum ECAP threshold was 1650 µA (No VNS range: 60 – 700 µA; VNS: 100 – 1650 µA), which was below the chronic stimulation level of 1.8 mA and confirmed stimulation was delivered at suprathreshold levels over the 4 weeks of implantation. The average latency for the ECAP response recorded on electrodes 3-4, positioned 4.5 mm from the stimulating electrodes 1-2 (**Figure 1A**), was 7.5 ± 0.46 ms in No VNS mice, corresponding to a conduction velocity of approximately 0.60 m/s. In VNS mice, the latency measured was 7.1 ± 0.40 ms, yielding an estimated conduction velocity of 0.63 m/s, indicating the ECAP population analyzed in this study fell within C-fiber conduction velocity range [39].

Differences between No VNS and VNS (Stimulation) groups and over Time were analyzed using a mixed-effects model (Time x Stimulation) due to missing values in the longitudinal data set (**Figure 5C, D**). Differences over Time between week 0 (pre-stim baseline) and all other timepoints were assessed using Dunnett's *post hoc* test. Differences between No VNS and VNS at each time point were assessed using Sidak's *post hoc* test.

Analysis of ECAP thresholds shows there was no significant interaction between Time X Stimulation on ECAP threshold ($F_{(2.1, 13.3)} = 1.84$; $p = 0.200$, **Figure 5C**). However, there was a significant main effect of Stimulation ($F_{(1, 11)} = 11.3$; $p = 0.006$; **Figure 5C**), indicating that the ECAP threshold from VNS mice was higher than from no VNS mice. There was also a main effect of Time ($F_{(2.1, 13.3)} = 5.14$; $p = 0.021$). A separate Main Effect of Time Dunnett's post hoc analysis showed that ECAP threshold of all electrodes significantly increased, compared to 0 week (baseline) thresholds at 2 weeks ($p = 0.004$) and 4 weeks ($p = 0.014$).

Analysis of ECAP peak amplitude show there was no significant interaction between Time X Stimulation on ECAP threshold ($F_{(2.2, 13.1)} = 0.7$; $p = 0.529$; **Figure 5D**). There was also no significant main effect of Stimulation ($F_{(1, 10)} = 0.06$; $p = 0.817$) or Time ($F_{(2.1, 13.1)} = 3.1$; $p = 0.078$; **Figure 5D**).

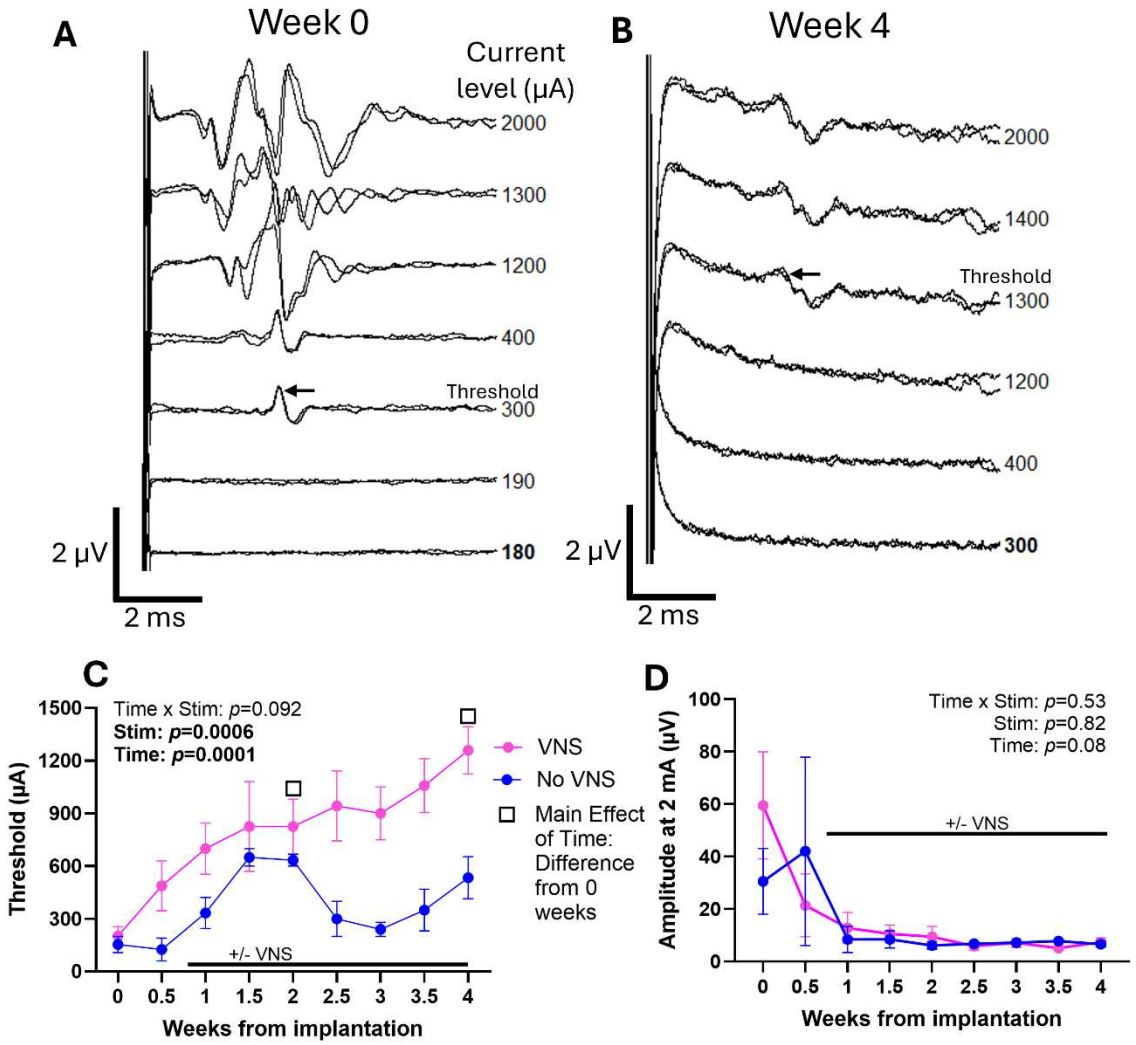



***Figure 5**. Changes in ECAP threshold during chronic implantation and stimulation. **A**: Representative ECAP waveforms taken at week 0, with an ECAP threshold of 300 μA indicated by 'arrow'. **B**: ECAP waveforms taken from the same stimulated (VNS) animal, showing an ECAP threshold of 1300 μA, as indicated by a black arrow. **C-D**: ECAP threshold (μA, **C**) and ECAP peak to peak amplitude (μV, **D**) over 4 weeks are shown in No VNS (unstimulated) and VNS (stimulated) mice. Data in C-D show mean ± SEM, a two-way mixed effects ANOVA was performed to assess the effect of Stimulation (stim) on ECAP threshold and amplitude between week 0 and 4. Significant differences indicated as '□' represents p<0.05 across all electrodes from week 0 value.*

## Electrical safety of chronic implantation and stimulation in mice

ECAP threshold was recorded twice a week over the 4 weeks following implantation, resulting in a total of *n*=77 ECAP recordings from *n*=13 mice. Specifically, there were *n*=24 ECAP thresholds recorded for no VNS cohort (*n*=3 mice) and *n*=53 ECAP thresholds recorded for

VNS cohort (*n*=9 mice). The minimum ECAP threshold charge required to evoke a neural response was plotted against the charge density over the 4 weeks of testing on a Shannon plot to assess whether the stimulation parameters approached tissue damage limits (**Figure 6**).

All ECAP thresholds (*n*=77) fell below the FDA approved upper safety limit of k=1.75 limit. Furthermore, all ECAP thresholds (*n*=77) were recorded below the water separation window (216 µC/cm$^2$/phase). A total of 97.4% (*n*=75 out of 77 ECAP thresholds) were recorded below k=1.5 safety limit. Only n=2 ECAP thresholds recorded from *n*=2 separate mice at 4 weeks following implantation were around the 1.5 safety limit (Mouse #7427: 210 µC/cm$^2$/phase; Mouse #7428: 204 µC/cm$^2$/phase; **Figure 6**).

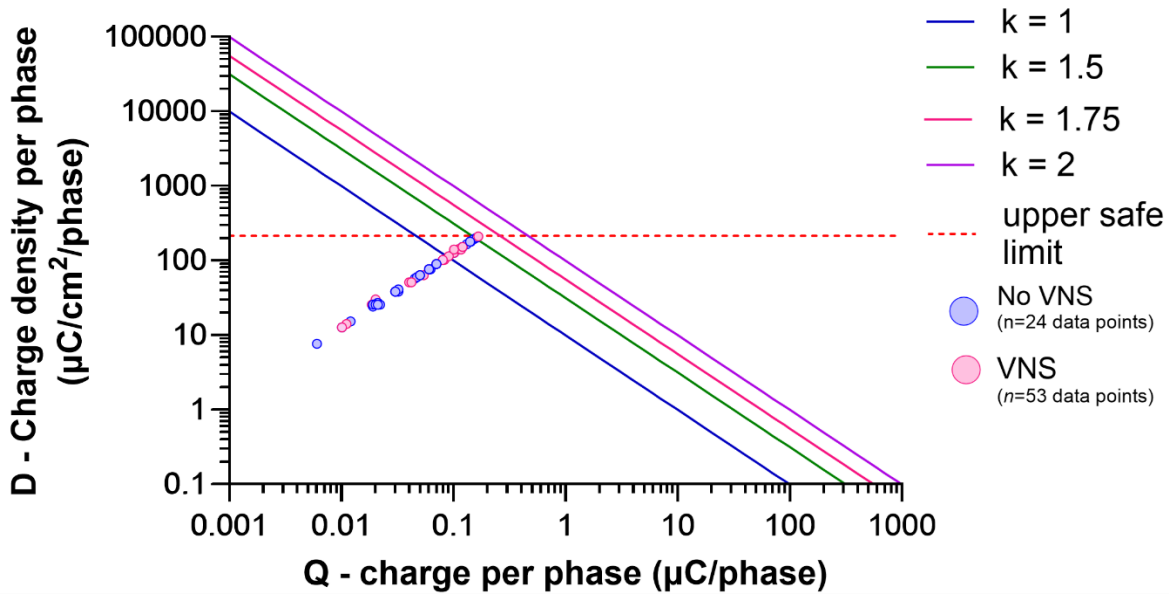



**Figure 6**. *Quantification of charge density per phase and charge per phase of during chronic implantation and stimulation. Data show individual values of every ECAP test conducted over 4 weeks in No VNS (n=3 mice; n=24 ECAP thresholds) and VNS (n=9 mice; n=53 ECAP thresholds) cohorts. The water window at 216 µC/cm/phase was indicated by a red dotted line, a k value of 1 indicated by a blue line, a k value of 1.5 by a green line, a k value of 1.75 a red line, and a k value of 2 indicated by a purple line. Collectively, these lines indicate safety limits.*

**Biological safety of chronic implantation and stimulation in mice**

Tolerability of chronic implantation and stimulation

*Implantation*: The implantation period for all mice (*n*=13) was 4 weeks, with no early terminations required (Table 1). Following implantation surgery, dorsal and abdominal skin incisions sites healed, with no infections and irritations seen around percutaneous pedestals (*n*=13). No adhesions to the abdominal wall were observed following termination and a macroscopic autopsy inspection. *Stimulation:* During chronic stimulation experiments, VNS was delivered (*n* = 7, Table 1) for a mean total of 43.4 ± 0.57 hrs over 14.6 ± 0.30 mean number of days (Table 1). No adverse responses, such as startling, agitation, or coughing were observed during VNS, and mice usually resumed normal calm feeding or sleeping behaviors. There were no differences in weight of mice in No VNS cohort (median +/- interquartile range (IQR): 24.5 g (24 – 25.8 g; *n* = 4) compared to VNS at the end of 4 weeks of chronic implantation and

stimulation (median +/- interquartile range (IQR): 26 g (25 – 26.8 g; $n$=9; Mann Whitney U test: $p$ = 0.12).

Effect of chronic implantation and stimulation on tissues and histopathology of the abdominal vagus nerve

*Autopsy observations of array in vivo*

Following 4 weeks of chronic implantation, a macroscopic examination of cutaneous and subcutaneous tissues surrounding the percutaneous connector showed good healing ($n$ = 13), despite tethering to a cable for on average 43.4 ± 0.57 hrs. over 14.6 ± 0.30 days (including No VNS mice). Minimal destruction to the percutaneous pedestal, due to animal chewing or scratching, was observed, and plugs generally remained intact and functional. The subcutaneous cable was encapsulated with a benign fibrosis tissue response, which provided stability to the cable positioning in the body. Within the abdominal cavity, examination of the custom vagus nerve array *in vivo* showed that a thin benign fibrous tissue encapsulation had formed (**Figure 1A, B**). The array remained anchored to and aligned with the esophagus, resulting in no twisting of the vagus nerve. Esophageal tissues that contacted the arrays via suturing appeared undamaged and free from macroscopic observations of infection or irritation. Furthermore, no irritation, prior hemorrhaging or hematomas developed from surgery, or abdominal tissue adhesions were observed in adjacent abdominal organs (esophagus, liver, intestines).

*Quantification of the abdominal vagus nerve*

Quantification of total fascicle area was conducted on abdominal anterior vagus nerves from normal (non-implanted) ($n$=10), chronically implanted no VNS mice ($n$=4) and chronically implanted and stimulated VNS mice ($n$=7; **Figure 7A**). In the VNS cohort, two samples (7427, #7431, Table 1 supplementary) were lost due to histological processing damage or errors. A one-way ANOVA was performed to determine the effects of chronic implantation and stimulation on total fascicle area (µm$^2$). There were no significant differences in total fascicle area of the anterior vagus nerve in normal, no VNS and VNS mice ($F_{(2, 18)}$ = 1.79; $p$=0.200, **Figure 7B**).

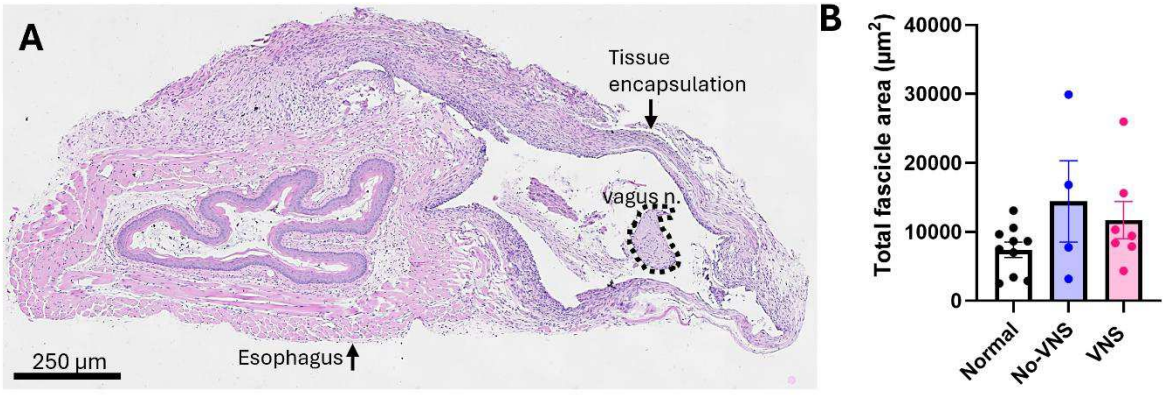



***Figure** 7. Quantification of the chronically implanted and stimulated abdominal anterior vagus nerve. **A**: Representative H&E image shows the chronically implanted and stimulated anterior vagus nerve and adjacent oesophagus from a mouse in the VNS cohort. **B**: Quantification of total fascicle area of the anterior vagus nerve from mice that were normal (n=10), or in No VNS (n=4) or VNS (n=7) cohorts. Data show mean ± SEM and a one-way*

*ANOVA was performed to assess the effects of chronic implantation and stimulation on fascicle area (μm²). Significant differences were indicated as '*' and accepted as p<0.05.*

# Discussion

The number of applications for VNS as a therapy of human disease is growing rapidly. Transgenic and disease-specific models in mice are essential for assessing the potential efficacy of VNS as a critical step for translation into humans. Here we show *in vitro* and *in vivo* electrochemical stability of electrodes from an abdominal vagus nerve array during chronic implantation and stimulation in the mouse. Although ECAP thresholds increased after 4 weeks of chronic stimulation and implantation, all activation thresholds ($n$=77, $n$=13 mice) remained below the FDA approved electrical safety limit (k=1.75) and water electrolysis window (216 μC/cm²/phase). Furthermore, stimulation was well tolerated by awake mice and there were no signs of histological damage. As such, we conclude that our miniaturized abdominal vagus nerve electrode array is a safe, well tolerated bioelectric technology platform that could be used to assess efficacy of VNS in a range of mouse models of human disease.

Electrode array design considerations

The small diameter of the mouse abdominal vagus nerve (~130 um), the fragility of the nerve and surrounding tissues, and the limited space available for implantation pose significant challenges for electrode array design[1]. Here we developed an extraneural two-pair cuff platinum electrode array embedded in medical grade silicone, which are biocompatible materials that have been used extensively in medical devices[40], as well as in our own abdominal VNS clinical trials (NCT07017686; NCT05469607). The surface area of the stimulating electrodes was calculated based on the electrical safe limit of k=1.75, which is a well-accepted safe stimulation limit below the typical threshold for tissue damage and allowed the theoretical safe delivery of 1.8 mA current at 100 μs pulse width or 180 nC charge. Another essential design feature was a second electrode pair placed at a specific distance (4.5 mm) to allow recording of ECAP responses within the C-fiber latency. This distance was precisely set to allow C-fiber waveforms to be recorded outside the stimulation artefact, which can often obscure responses (**Fig 4A**, **B**). However, C-fibers of the abdominal vagus nerve have slow conduction velocities (0.2 – 2 m/s), are poorly synchronized and response amplitudes are diminished with increasing distance between the stimulating and recording electrodes. Here we found a distance between stimulating and recording electrode pairs of 4.5 mm appropriate to satisfy both requirements. Recording ECAPs confirms correct placement of the array around the nerve and that therapy is being delivered suprathreshold and has been used extensively in our abdominal VNS efficacy research in rat[14,41,42], sheep[43] and human (NCT07017686; NCT05469607).

Electrochemical changes *in vitro*

There was no effect on EIS measurements in vitro, indicating the stability of intrinsic electrochemical properties of the electrode. However, there was a significant increase in *in vitro* CSC values between pre- and post-implantation values of stimulated electrodes potentially indicating a stimulation-induced expansion of the effective surface area of Stim electrodes [45]. Importantly, there were no changes to *in vitro* Stim electrode CIL values indicating that the potential increase in effective surface area did not change how much electrical charge can safely be applied to the electrode without crossing the water electrolysis window [45]. There were no effects of chronic implantation and stimulation on CG impedance, however group (i.e. pre and post) differences between passive and no stim electrodes are suggestive of manufacturing differences.

Electrochemical changes *in vivo*

There was no effect of stimulation on the EIS impedance at 100 Hz, 1 kHz and 10 kHz over 4 weeks. However, there were changes in 100Hz and 10 kHz impedance across all electrodes over time which likely reflects tissue encapsulation. However, the level of tissue encapsulation was not affected by the presence of stimulation, indicated by no significant differences in EIS impedance between electrode conditions. CSC data shows an initial transient decrease in CSC measurements, which returned to baseline levels from week 2.5 to 4 weeks. The transient decrease in CSC values is due to a decrease in the active surface area potentially caused by biofouling from tissue encapsulation known to occur within the first few weeks of implantation. Although there was a Main effect of electrode condition, no significant difference were revealed in the post hoc analysis making this a result difficult to draw any conclusions from. Nevertheless, there was a trend increase in CSC for the Stim electrodes, which is consistent with the CSC *in vitro* results, indicating an expansion of the effective surface area. There were no differences in CIL values between passive and no stim or stim electrode groups, suggesting that chronic stimulation did not alter the electrodes' safe charge-transfer capacity or water electrolysis window [46]. At 0.5 weeks, CG impedance of passive electrodes was significantly higher than that of no stim and stim electrode. This finding, coupled with the in pre-implantation in vitro suggests there may of have been inherent small manufacturing differences between the passive and no stim / stim electrodes. Stim electrode CG remained significantly less than passive electrode CG from 1.5 weeks onwards during chronic implantation. The lower common-ground impedance of stim electrodes compared with passive electrodes is consistent with a stimulation-mediated electrode-cleaning effect, potentially through reduced protein or cellular accumulation and improved ionic access to the platinum electrode surface [47]. The absence of a corresponding change in charge injection limit between stim and passive electrodes also suggests that this effect did not materially alter the electrodes' safe charge-transfer capacity. Transient increases in CG impedance of passive and no stim electrodes was likely due to the fibrotic tissue response, causing increase in tissue density at the interface, as well as biofouling [44,45]. In summary, the observed changes in *in vivo* electrochemical measurements and common-ground impedance likely reflected biofouling and changes at the tissue interface, without affecting safe charge-injection limits.

Biological safety of chronic implantation and stimulation

During chronic implantation and stimulation of the abdominal VNS device, there were no adverse events, weight loss, macroscopic signs of infection or abhorrent behavior related to the onset of VNS, suggesting the device was well tolerated by the mice. The abdominal vagus nerve is very small (approximately 130 μm in diameter) and fragile, making it susceptible to injury from surgical manipulation, chronic implantation, and unsafe high charge densities delivered during chronic stimulation[1]. Damage to axons causes disruptions to axonal transport, the functionality of the nerve and can lead to neural degeneration [48]. Here we show that ECAP thresholds were recorded on week 4 in a majority of mice ($n$=9 out of 11), suggesting most nerves remained physiologically functional. The n=2 animals that did not have ECAPs were likely due to the nerve slipping out of the channel, confirmed postmortem. Although ECAP thresholds were significantly higher in VNS mice than No VNS mice, a similar pattern also observed in a VNS sheep safety study [43], thresholds always remained below 1.8 mA stimulation level. We also observed a (non-significant) decrease in maximum ECAP amplitude between early weeks (week 0 to 0.5) and later weeks (1 – 4 weeks), which may be due to foreign body response building up at the electrode-nerve interface, evidenced by electrochemical changes and in the histology (**Figure 6A**). However, although maximum ECAP amplitude decreases initially, they remain unchanged from week 1 to 4, indicating stability of the electrode-tissue interface. Quantitative assessment of histology shows no changes in abdominal vagus nerve

total fascicle area after chronic implantation and stimulation suggesting no signs of axonal degeneration. In summary, the VNS device was well tolerated, and the implanted nerve remained undamaged and functional.

Electrical safety of chronic stimulation

Here we applied chronic abdominal VNS at 180 nC/phase at a charge density of 5225229 uC/cm$^2$, which was close to the upper k=1.75 Shannon limit, an equation used to define the boundary between safe and tissue damaging levels of electrical stimulation. In this study, we confirm that 100% of stimulation ECAP thresholds in all stimulated and unstimulated mice tested over 4 weeks of chronic implantation (n=77 ECAP recordings over 4 weeks from n=11 mice) remained below the k=1.75 electrical safety limit. The k=1.75 safety limit [12] is commonly used as an empirical benchmark of FDA regulated devices for assessing risk of neural tissue damage from electrical stimulation [49]. The electrochemical water window is another measure of tissue safety that measures the limit at which electrode charge transfer become imbalanced, resulting in irreversible faradaic reactions cause significant electrolysis of water, corrosion of electrode material and chloride ion oxidation [28,50]. However, all ECAP thresholds recorded remained below the water separation window (216 μC/cm$^2$/phase). At unsafe charge densities higher than k=1.75 of the Shannon limit or above the water window (216 μC/cm$^2$/phase), platinum electrodes can undergo irreversible faradaic reactions resulting in dissolution of the platinum electrode and oxidation of chloride ions [44]. The formation of platinum electrode corrosion alters the geometry of the electrode surface area, which will be reflected in changes to electrochemical tests such as the CSC, CI and impedance.

Clinical relevance

Our laboratory has used rat and sheep models to show safety and efficacy of abdominal VNS treatment, which has directly led to clinical trials for inflammatory bowel disease and rheumatoid arthritis. The clinical importance of this technology lies in its ability to support the assessment of abdominal VNS efficacy in mouse models for other chronic inflammatory diseases, such as ankylosing spondylitis, psoriasis and pancreatitis [51-53]. Here we assessed safety and device functionality over four-weeks, which is in line with the timeline of many efficacy studies in inflammatory disease mouse models. However, future studies could consider expanding this timeframe to 3 months which would be in line with longer term metabolic disease models [12,54].

## Conclusion

In conclusion, this study establishes the array as a safe peripheral nerve interface for awake, chronic stimulation of the abdominal vagus nerve in mice. This bioelectric technology platform allows the assessment of efficacy, and understanding of VNS-driven mechanisms, in a large range of available transgenic and disease-specific models, thereby potentially broadening the application of VNS as a treatment of human disease.

## Acknowledgements

We would like to acknowledge Ms Amy Morley, Ms Philippa Kammerer, Ms. Monireh Amerion, Ms. Ella Trang, and A/Prof Peta Grigsby for laboratory and technical assistance.

## Author contributions

All authors made substantial, direct and intellectual contributions to the work. RK conducted all experiments, analyzed the data and was the primary writer of the manuscript (MS). TH performed the world-first abdominal VNS implant surgeries, advised on electrochemical testing and revised the MS. JZ manufactured the custom electrodes and revised the MS sections

on array fabrication. JBF contributed expertise in study concept and design and analysis, and substantially revised the MS. SCP identified the gap in the field, advised on experimental design and analysis, and substantially revised the MS.

## Ethics statement

All animal procedures were approved by the Animal Research and Ethics Committee of St. Vincent's Hospital (reference number.: 13.24) and complied with the Australian Code for the Care and Use of Animals for Scientific Purposes (National Health and Medical Research Council of Australia).

## Funding

This research was funded in whole or part by the National Health and Medical Research Council (ROR https://ror.org/011kf5r70) [2028605]. For the purposes of open access, the author has applied a CC BY public copyright license to any Author Accepted Manuscript version arising from this submission. The Bionics Institute also acknowledges the support they receive from the Victorian Government through its Operational Infrastructural Support Program

## Data availability

The data that support the findings of this study are available from the corresponding author upon request.

## Disclosures

All authors declare no conflicts of interest, financial or otherwise.

# Supplementary

***Table 1.*** *Summary of animal used, stimulation received and other measurements taken. Animals that were tethered but received no VNS were termed the 'no VNS' cohort, while animals that received stimulation were termed the 'VNS cohort. The 'Y' indicates 'yes' and 'N' indicates 'no'.*

| Animal ID | Implant duration (days) | Time stimulated (hrs / days) | Charge (µC) | Charge density (µC/cm²) | ECAPs in week 4 | Histology | Comment |
|---|---|---|---|---|---|---|---|
| **No VNS #1 (#7027)** | 28 | N/A | 0 µC | N/A | Y | Y | |
| **No VNS #2 (#7028)** | 28 | N/A | 0 µC | N/A | Y | Y | |
| **No VNS #3 (#7320)** | 28 | N/A | 0 µC | N/A | Y | Y | |
| **No VNS #4 (#7321)** | 28 | N/A | 0 µC | N/A | Y | Y | |
| **VNS#1 (#7362)** | 28 | 45 / 15 | 180 µC | 5225229 | Y | Y | |
| **VNS#2 (#7363)** | 28 | 45 / 15 | 180 µC | 5225229 | N | Y | Nerve not in channel |
| **VNS#3 (7029)** | 28 | 45 / 15 | 180 µC | 5225229 | N | Y | Nerve not in channel |
| **VNS#4 (7030)** | 28 | 45 / 15 | 180 µC | 5225229 | Y | Y | |
| **VNS#5 (7427)** | 28 | 42.2 / 14 | 180 µC | 5225229 | Y | N | Nerve lost in processing |
| **VNS#6 (7428)** | 28 | 42.3 / 14 | 180 µC | 5225229 | Y | Y | |
| **VNS#7 (7429)** | 28 | 42.2 / 14 | 180 µC | 5225229 | Y | Y | |
| **VNS#8 (7430)** | 28 | 42.2 / 14 | 180 µC | 5225229 | Y | Y | |
| **VNS#9 (7431)** | 28 | 45.2 / 16 | 180 µC | 5225229 | Y | N | No in vitro data; Nerve lost in processing |
| **Average** | | | | | | | |
| **No VNS** (***n***=4) | 28<br>28 | VNS | VNS<br>180 µC | | | | |
| **VNS** (***n***=9) | | 43.4 ± 0.57<br>14.6 ± 0.30 | | | | | |

# References


1 Larson, C. E. & Meng, E. A review for the peripheral nerve interface designer. *J Neurosci Methods* **332**, 108523 (2020). https://doi.org/http://doi.org/10.1016/j.jneumeth.2019.108523

2 Pavlov, V. A., Chavan, S. S. & Tracey, K. J. Bioelectronic medicine: From preclinical studies on the inflammatory reflex to new approaches in disease diagnosis and treatment. *Cold Spring Harb Perspect Med* **10** (2020). https://doi.org/10.1101/cshperspect.a034140

3 Tracey, K. J. The inflammatory reflex. *Nature* **420**, 853-859 (2002). https://doi.org/10.1038/nature01321

4 Administration, U. S. F. a. D. *Summary of Safety and Effectiveness Data (SSED) - VNS Therapy System (PMA : P970003/S207)*, <https://www.accessdata.fda.gov/cdrh_docs/pdf/P970003S207B.pdf> (2017).

5 Administration, U. S. F. a. D. *Summary of Safety and Effectiveness Data (SSED) - VNS Therapy System (PMA : P970003/S50)*, <https://www.accessdata.fda.gov/cdrh_docs/pdf/P970003S050B.pdf> (2005).

6 Administration, U. S. F. a. D. *Summary of Safety and Effectiveness Data (SSED) - SetPoint System (PMA : P240039)*, <https://www.accessdata.fda.gov/cdrh_docs/pdf24/P240039B.pdf> (2025).

7 Bonaz, B. *et al.* Chronic vagus nerve stimulation in Crohn's disease: a 6-month follow-up pilot study. *Neurogastroenterology & Motility* **28**, 948-953 (2016). https://doi.org/https://doi.org/10.1111/nmo.12792

8 D'Haens, G. *et al.* Neuroimmune Modulation Through Vagus Nerve Stimulation Reduces Inflammatory Activity in Crohn's Disease Patients: A Prospective Open-label Study. *Journal of Crohn's and Colitis* **17**, 1897-1909 (2023). https://doi.org/10.1093/ecco-jcc/jjad151

9 Sinniger, V. *et al.* A 12-month pilot study outcomes of vagus nerve stimulation in Crohn's disease. *Neurogastroenterol Motil* **32**, e13911 (2020). https://doi.org/10.1111/nmo.13911

10 Zaaimi, B. *et al.* Vagus Nerve Stimulation Induces Concomitant Respiratory Alterations and a Decrease in SaO2 in Children. *Epilepsia* **46**, 1802-1809 (2005). https://doi.org/https://doi.org/10.1111/j.1528-1167.2005.00283.x

11 Khurana, D. S. *et al.* Vagus nerve stimulation in children with refractory epilepsy: unusual complications and relationship to sleep-disordered breathing. *Child's Nervous System* **23**, 1309-1312 (2007). https://doi.org/10.1007/s00381-007-0404-8

12 Kalagara, R. *et al.* Complications of Implanted Vagus Nerve Stimulation: A Systematic Review and Meta-Analysis. *Cerebrovascular Diseases* **54**, 112-120 (2024). https://doi.org/10.1159/000536362

13 Hyakumura, T., Payne, S. C., Matarazzo, J. V., Adams, W. K. & Fallon, J. B. Abdominal Vagus Nerve Stimulation Increases Firing in the Rat Locus Coeruleus. *Neuromodulation: Technology at the Neural Interface* **28**, 1239-1247 (2025). https://doi.org/https://doi.org/10.1016/j.neurom.2025.05.003

14 Payne, S. C. *et al.* Anti-inflammatory effects of abdominal vagus nerve stimulation on experimental intestinal inflammation. *Front Neurosci* **13**, 418 (2019). https://doi.org/http://doi.org/10.3389/fnins.2019.00418

15 Payne, S. C. *et al.* Vagus nerve stimulation to treat inflammatory bowel disease: a chronic, preclinical safety study in sheep. *Bioelectronics in Medicine* **1**, 235-250 (2018). https://doi.org/10.2217/bem-2018-0011

16 Payne, S. C., Romas, E., Hyakumura, T., Muntz, F. & Fallon, J. B. Abdominal vagus nerve stimulation alleviates collagen-induced arthritis in rats. *Frontiers in Neuroscience* **16** (2022). https://doi.org/10.3389/fnins.2022.1012133
17 Bedell, M., Jenkins, N. & Copeland, N. Mouse models of human disease. Part I: techniques and resources for genetic analysis in mice. *Genes & Development* **11**, 1-10 (1997). https://doi.org/10.1101/gad.11.1.1
18 Association, E. A. R. *Mice and animal research*, <https://www.eara.eu/mice-and-animal-research> (2023).
19 Bryda, E. C. The Mighty Mouse: the impact of rodents on advances in biomedical research. *Mo Med* **110**, 207-211 (2013).
20 Stakenborg, N. *et al.* Comparison between the cervical and abdominal vagus nerves in mice, pigs, and humans. *Neurogastroenterol Motil* **32**, e13889 (2020). https://doi.org/10.1111/nmo.13889
21 Majji, A. B. *et al.* Long-term histological and electrophysiological results of an inactive epiretinal electrode array implantation in dogs. *Invest Ophthalmol Vis Sci* **40**, 2073-2081 (1999).
22 Niparko, J. K., Altschuler, R. A., Xue, X. L., Wiler, J. A. & Anderson, D. J. Surgical implantation and biocompatibility of central nervous system auditory prostheses. *Ann Otol Rhinol Laryngol* **98**, 965-970 (1989). https://doi.org/10.1177/000348948909801209
23 Robblee, L. S., Lefko, J. L. & Brummer, S. B. Activated Ir: An electrode suitable for reversible charge injection in saline solution. *Journal of The Electrochemical Society* **130**, 731-733 (1983). https://doi.org/10.1149/1.2119793
24 Rose, T. L. & Robblee, L. S. Electrical stimulation with Pt electrodes. VIII. Electrochemically safe charge injection limits with 0.2 ms pulses (neuronal application). *IEEE Transactions on Biomedical Engineering* **37**, 1118-1120 (1990). https://doi.org/10.1109/10.61038
25 White, R. L. & Gross, T. J. An Evaluation of the Resistance to Electrolysis of Metals for Use in Biostimulation Microprobes. *IEEE Transactions on Biomedical Engineering* **BME-21**, 487-490 (1974). https://doi.org/10.1109/TBME.1974.324339
26 Cogan, S. F. Neural Stimulation and Recording Electrodes. *Annual Review of Biomedical Engineering* **10**, 275-309 (2008). https://doi.org/https://doi.org/10.1146/annurev.bioeng.10.061807.160518
27 Brummer, S. & Turner, M. J. Electrochemical Considerations for Safe Electrical Stimulation of the Nervous System with Platinum Electrodes. *IEEE Transactions on Biomedical Engineering* **BME-24**, 59-63 (1977).
28 Huang, C. Q., Carter, P. M. & Shepherd, R. K. Stimulus induced pH changes in cochlear implants: An in vitro and in vivo study. *Ann Biomed Eng* **29**, 791-802 (2001).
29 Grill, W. M. Safety considerations for deep brain stimulation: review and analysis. *Expert Review of Medical Devices* **2**, 409-420 (2005). https://doi.org/10.1586/17434440.2.4.409
30 Merrill, D. R., Bikson, M. & Jefferys, J. G. R. Electrical stimulation of excitable tissue: design of efficacious and safe protocols. *Journal of Neuroscience Methods* **141**, 171-198 (2005). https://doi.org/https://doi.org/10.1016/j.jneumeth.2004.10.020
31 Cogan, S. F., Ludwig, K. A., Welle, C. G. & Takmakov, P. Tissue damage thresholds during therapeutic electrical stimulation. *J. Neural. Eng.* **13**, 021001 (021013 pp) (2016). https://doi.org/10.1088/1741-2560/13/2/021001
32 Shannon, R. V. A model of safe levels for electrical stimulation. *IEEE Trans. Biomed. Eng.* **39**, 424-426 (1992). https://doi.org/10.1109/10.126616

33 Hyakumura, T., Fallon, J. B. & Payne, S. C. Implantation surgery for abdominal vagus nerve stimulation and recording studies in awake rats. *J Vis Exp* (2024). https://doi.org/10.3791/65896

34 Matarazzo, J. V., Williams-Wynn, D. T., Fallon, J. B. & Payne, S. C. Magnetically Coupled Percutaneous Connector for Chronic Electrical Peripheral Nerve Stimulation and Recording in Awake Rats. *IEEE Trans Biomed Eng* **72**, 35-42 (2025). https://doi.org/10.1109/tbme.2024.3436649

35 Fallon, J. B., Senn, P. & Thompson, A. C. in *Neural Interfaces Conferences* (Minneapolis, MN, 2018).

36 Hyakumura, T. *et al.* Improving deep brain stimulation electrode performance in vivo through use of conductive hydrogel coatings. *Front Neurosci* **15**, 761525 (2021). https://doi.org/10.3389/fnins.2021.761525

37 Fallon, J. B. & Payne, S. C. Electrophysiological recording of electrically-evoked compound action potentials. *io.protocols* (2020). https://doi.org/http://dx.doi.org/10.17504/protocols.io.bfwyjpfw

38 Schindelin, J. *et al.* Fiji: an open-source platform for biological-image analysis. *Nature Methods* **9**, 676-682 (2012). https://doi.org/10.1038/nmeth.2019

39 Castoro, M. A. *et al.* Excitation properties of the right cervical vagus nerve in adult dogs. *Exp. Neurol.* **227**, 62-68 (2011). https://doi.org/10.1016/j.expneurol.2010.09.011

40 Clark, G. M., Shepherd, R. K., Patrick, J. F., Black, R. C. & Tong, Y. C. Design and fabrication of the banded electrode array. *Ann. N. Y. Acad. Sci.* **405**, 191-201 (1983).

41 Payne, S. C., Romas, E., Hyakumura, T., Muntz, F. & Fallon, J. B. Abdominal vagus nerve stimulation alleviates collagen-induced arthritis in rats. *Front Neurosci* **16**, 1012133 (2022). https://doi.org/10.3389/fnins.2022.1012133

42 Payne, S. C. *et al.* Blood glucose modulation and safety of efferent vagus nerve stimulation in a type 2 diabetic rat model. *Physiol Rep* **10** (2022). https://doi.org/http://doi.org/10.14814/PHY2.15257

43 Payne, S. C. *et al.* Vagus nerve stimulation to treat inflammatory bowel disease: a chronic, preclinical safety study in sheep. *Bioelectron Med* **1**, 235-250 (2018). https://doi.org/http://doi.org/10.2217/bem-2018-0011

44 Shepherd, R. K. *et al.* Chronic intracochlear electrical stimulation at high charge densities: reducing platinum dissolution. *Journal of Neural Engineering* **17**, 056009 (2020). https://doi.org/10.1088/1741-2552/abb7a6

45 Dalrymple, A. N. *et al.* Electrochemical and biological characterization of thin-film platinum-iridium alloy electrode coatings: a chronic in vivo study. *J Neural Eng* **17**, 036012 (2020). https://doi.org/10.1088/1741-2552/ab933d

46 Vatsyayan, R. & Dayeh, S. A. A universal model of electrochemical safety limits in vivo for electrophysiological stimulation. *Frontiers in Neuroscience* **Volume 16 - 2022** (2022). https://doi.org/10.3389/fnins.2022.972252

47 Newbold, C. *et al.* Changes in biphasic electrode impedance with protein adsorption and cell growth. *J Neural Eng* **7**, 056011 (2010). https://doi.org/10.1088/1741-2560/7/5/056011

48 Conforti, L., Gilley, J. & Coleman, M. P. Wallerian degeneration: an emerging axon death pathway linking injury and disease. *Nat Rev Neurosci* **15**, 394-409 (2014). https://doi.org/10.1038/nrn3680

49 Kumsa, D. *et al.* Public Regulatory Databases as a Source of Insight for Neuromodulation Devices Stimulation Parameters. *Neuromodulation* **21**, 117-125 (2018). https://doi.org/10.1111/ner.12641

50 Brummer, S. B., McHardy, J. & Turner, M. J. Electrical stimulation with Pt electrodes: Trace analysis for dissolved platinum and other dissolved electrochemical products. *Brain Behav Evol* **14**, 10-22 (1977). https://doi.org/10.1159/000124611

51 Alliance for Advancing Bioelectronic, M. Building a bioelectronic medicine movement 2019: insights from leaders in industry, academia, and research. *Bioelectron Med* **6**, 1 (2020). https://doi.org/10.1186/s42234-020-0037-8

52 Cracchiolo, M. *et al.* Bioelectronic medicine for the autonomic nervous system: clinical applications and perspectives. *J Neural Eng* **18**, 1002 (2021). https://doi.org/http://doi.org/10.1088/1741-2552/abe6b9

53 Eberhardson, M., Tarnawski, L., Centa, M. & Olofsson, P. S. Neural Control of Inflammation: Bioelectronic Medicine in Treatment of Chronic Inflammatory Disease. *Cold Spring Harb Perspect Med* **10** (2020). https://doi.org/10.1101/cshperspect.a034181

54 Kleinert, M. *et al.* Animal models of obesity and diabetes mellitus. *Nature Reviews Endocrinology* **14**, 140-162 (2018). https://doi.org/10.1038/nrendo.2017.161